

Leading fermionic three-loop corrections to electroweak precision observables

Lisong Chen, Ayres Freitas

Pittsburgh Particle-physics Astro-physics & Cosmology Center (PITT-PACC)
 Department of Physics & Astronomy, University of Pittsburgh, Pittsburgh, PA 15260, USA
 afreitas@pitt.edu
 lic114@pitt.edu

October 29, 2021



*15th International Symposium on Radiative Corrections:
 Applications of Quantum Field Theory to Phenomenology,
 FSU, Tallahassee, FL, USA, 17-21 May 2021*
 doi:[10.21468/SciPostPhysProc.7.1.011](https://doi.org/10.21468/SciPostPhysProc.7.1.011)

Abstract

In this proceeding, we highlight the computation of leading fermionic three-loop corrections to electroweak precision observables (EWPOs) accomplished recently. We summarize the numerical analysis and provide an outlook.

Contents

1	Introduction	2
2	Renormalization	2
2.1	Renormalization Schemes	2
2.2	EWPOs definitions	4
2.2.1	Fermi constant G_μ	4
2.2.2	Effective weak mixing angle $\sin^2\theta_{eff}^f$	4
2.2.3	Partial Width $\bar{\Gamma}[Z \rightarrow f\bar{f}]$	5
3	Technical Aspects	5
4	Numerical Results	6
5	Conclusions	7
	References	8

1 Introduction

The electroweak precision observables (EWPOs) are a group of quantities associated with the properties of the Z and W bosons. They can be obtained from measurements of processes mediated by W and Z bosons, where the experimentally irreducible background has been carefully removed. The EWPOs, as one of the most crucial testbeds of the Standard Model (SM), played a key role in the physics program of LEP and SLC and they will be further scrutinized at future high-luminosity e^+e^- colliders, such as FCC-ee, ILC, CLIC, and CEPC, with substantially improved precision. One can only fully take advantage of these high-precision measurements with accurate theoretical predictions whose uncertainties are well-controlled. The latter require calculations of multi-loop radiative corrections together with the better knowledge of theory input parameters. Up till now, the theoretical predictions of the EWPOs, such as (i) the W-boson mass M_W , (ii) the partial widths of the Z-boson Γ_f , and (iii) the effective weak mixing angle $\sin^2 \theta_{eff}^f$, have been known up to full two-loop level [1–10], and partial three- and four-loop level contributions given by top Yukawa coupling enhancement [11–13] within the SM. All these corrections amount to predictions with theoretical uncertainties being safely below the current experimental precision (see Ref [14–16] for detailed reviews). Yet the expected precision of future e^+e^- colliders impose the need of computing three and four-loop corrections at full EW $\mathcal{O}(\alpha^3)$ and mixed EW-QCD $\mathcal{O}(\alpha^2\alpha_s)$ and $\mathcal{O}(\alpha\alpha_s^2)$. In this proceeding, we survey the recently accomplished calculations of leading fermionic three-loop corrections to EWPOs at full EW $\mathcal{O}(\alpha^3)$ and mixed EW-QCD $\mathcal{O}(\alpha^2\alpha_s)$, where “leading fermionic” refers to the maximal number of closed fermionic loops at given orders. In sec. 2, we introduce the renormalization procedures for cases with and without QCD contributions. Sec. 3 highlights the technical aspects including the derivative and evaluation of the master integral (MI) and the computer algebra tools we used. One can find numerical results and shed light on future projections thereby in sec. 4 and the Conclusion, respectively.

2 Renormalization

2.1 Renormalization Schemes

We adopted the on-shell (OS) renormalization scheme for all electroweak radiative corrections. For corrections involving QCD, such as the case of leading fermionic three-loop at $\mathcal{O}(\alpha^2\alpha_s)$, where the top-quark mass receives radiative corrections from gluon exchange, we use OS scheme and modified minimal subtraction scheme ($\overline{\text{MS}}$) alternately to describe the renormalized top-quark mass. The reason for using both schemes is the following: the OS top mass definition is subject to the renormalon ambiguity from which the $\overline{\text{MS}}$ top-quark mass prescription is exempt. The $\overline{\text{MS}}$ top-quark mass prescription is thus preferable in practical calculations, yet an extra step is required to relate the $\overline{\text{MS}}$ value to an observable. These two schemes are related by a finite function, which has been carried out up to four-loop level [19]. The results carried out in both schemes after summing up all orders in perturbation theory should converge up to non-perturbative effects, and our numerical comparison between two schemes will reveal an inkling of it (see 4).

In the OS scheme, the physical mass of the massive unstable particle is defined to be the real part of the complex pole of the propagator, while the width is proportional to the imaginary part of the pole as follows,

$$s_0 \equiv \overline{M}^2 - i\overline{M}\Gamma, \quad (1)$$

The figure shows two rows of Feynman diagrams representing self-energy corrections. The top row, labeled $\Sigma_{V_1 V_2}(\alpha^3)$, contains three diagrams: a fermion loop with a gauge boson exchange and a blue 'x' counterterm, a fermion loop with a gauge boson exchange and a blue 'o' counterterm, and a fermion loop with a gauge boson exchange and a blue 'x' counterterm. The bottom row, labeled $\Sigma_{V_1 V_2}(\alpha_s \alpha^2)$, contains four diagrams: a fermion loop with a gluon exchange and a red 'x' counterterm, a fermion loop with a gluon exchange and a red 'o' counterterm, a fermion loop with a gluon exchange and a red 'x' counterterm, and a fermion loop with a gluon exchange and a red 'o' counterterm, followed by an ellipsis.

Figure 1: Diagrammatic 1-PI leading fermionic self-energy functions at different orders. V_1 and V_2 denote the possible different in- and outgoing gauge bosons. Vertices "o" and "x" indicate the counterterms at the loop order $\mathcal{O}(\alpha_s \alpha)$ or $\mathcal{O}(\alpha^2)$, and $\mathcal{O}(\alpha)$ or $\mathcal{O}(\alpha_s)$, distinguished by red (with QCD) and blue (without QCD), respectively.

where \bar{M} is the renormalized mass defined to be on-shell and the $\bar{\Gamma}$ is the width.¹ For a massive gauge boson, by requiring the inverse of Dyson re-summed two-point function to be zero at the pole as

$$D(s) = Z(s - \bar{M}^2) - \delta \bar{M}^2 Z + \Sigma(s)|_{s=s_0} \equiv 0, \quad (2)$$

we get the renormalization conditions

$$\delta \bar{M}^2 = Z^{-1} \Re \Sigma(\bar{M}^2 - i\bar{M}\bar{\Gamma}) \quad (3)$$

$$\bar{\Gamma} = \frac{\Im \Sigma(\bar{M}^2 - i\bar{M}\bar{\Gamma})}{ZM} \quad (4)$$

When deriving the renormalization condition for the Z boson, a more subtle complexity emerges from taking $\gamma - Z$ mixing effect into account (see detailed discussion in Ref. [20]). The renormalization conditions for massive fermions, akin to massive gauge boson cases, can also be obtained through $D_\psi(\not{p})|_{p^2=M_\psi^2 - iM_\psi\Gamma_\psi} = 0$, where D_ψ is the inverse of fermion two-point function written as

$$D_\psi(p) = Z_\psi(\not{p} - M_\psi) + \Sigma_\psi(p^2) - Z_\psi \delta M_\psi. \quad (5)$$

Hence we get the top-quark mass counterterm and width as

$$\begin{aligned} \delta M_\psi u(p) &= Z_\psi^{-1} \Re \Sigma_\psi(\not{p})u(p)|_{p^2=M_\psi^2 - iM_\psi\Gamma_\psi} \\ \Gamma_\psi u(p) &= Z_\psi^{-1} 2\Im \Sigma_\psi(\not{p})u(p)|_{p^2=M_\psi^2 - iM_\psi\Gamma_\psi}. \end{aligned} \quad (6)$$

By recursively applying the renormalization conditions eq. (3) eq. (4), we can obtain widths and mass counterterms in terms of 1-PI self-energies up to arbitrary orders (see explicit expressions in Ref. [20]). Since all EWPOs we want to compute are extracted from processes where the massive gauge bosons appear to be intermediate states only, the final results should be independent of field strength renormalization constants (we have checked it explicitly in our calculations). It is thus safe to set Z to be 1 in our cases.

In the $\overline{\text{MS}}$ scheme, the mass counterterm is meant to subtract the ultraviolet divergent piece along with constants $\log(4\pi)$ and γ_E . At one-loop QCD level, it is

$$\delta m_t = -\frac{3C_F g_s^2}{16\pi^2} \left(\frac{1}{\epsilon} + \log 4\pi - \gamma_E \right) m_t(\mu). \quad (7)$$

¹The mass and width defined here are theoretically well-defined and gauge-invariant [17], but the experimental mass and width M, Γ used, are related to $\bar{M}, \bar{\Gamma}$ by the relations $\bar{M} = M/\sqrt{1 + \Gamma^2/M^2}$, $\bar{\Gamma} = \Gamma/\sqrt{1 + \Gamma^2/M^2}$ [18].

And it relates to the OS top-quark mass by

$$\frac{M_t}{m_t} = 1 + \frac{\alpha_s C_F}{4\pi} \left(3 \log \frac{M_t^2}{\mu^2} - 4 \right) + \mathcal{O}(\alpha_s^2). \quad (8)$$

at one-loop level in QCD. Moreover, the renormalized weak mixing angle is defined by demanding that the relation $\sin^2 \theta_W = 1 - \overline{M}_W^2 / \overline{M}_Z^2$ holds to all orders. The electromagnetic charge, as a fundamental parameter, is renormalized to the coupling strength in Thompson scattering. Due to the non-perturbative contribution of light-quark fermionic loops at zero momentum in the Thompson limit, this contribution, parametrized as $\Delta\alpha_{had}$, is usually extracted from measurements of $e^+e^- \rightarrow hadrons$ [25].

2.2 EWPOs definitions

2.2.1 Fermi constant G_μ

The Fermi constant can be precisely obtained from muon decay. In the SM, it is defined as

$$G_\mu = \frac{\pi\alpha}{\sqrt{2}s_w^2 \overline{M}_W^2} (1 + \Delta r), \quad (9)$$

where all QED contributions have already been taken into account in the determination of G_μ from the muon lifetime. Here Δr features all higher-order corrections at the orders that we are interested in. This relation can be used to iteratively to determine the W-boson mass within the SM:

$$\overline{M}_W^2 = \overline{M}_Z^2 \left(\frac{1}{2} + \sqrt{\frac{1}{4} - \frac{\alpha\pi}{\sqrt{2}G_\mu \overline{M}_Z^2} (1 + \Delta r)} \right) \quad (10)$$

2.2.2 Effective weak mixing angle $\sin^2 \theta_{eff}^f$

The effective weak mixing angle is defined as associated with the ratio of the Z-boson vector coupling form factor and the axial-vector coupling form factor. It is most sensitively determined at the Z-pole where the Z/γ^* interference and photon exchange are suppressed. Hence we are interested in computing

$$\sin^2 \theta_{eff}^f = \frac{1}{4|Q_f|} \left(1 + \Re \frac{V_f(s)}{A_f(s)} \right) \Bigg|_{s=\overline{M}_Z^2}, \quad (11)$$

where

$$\begin{aligned} V_f(s) &= v_f^Z(s) - v_f^\gamma \frac{\Sigma_{\gamma Z}(s)}{s + \Sigma_{\gamma\gamma}(s)} \\ A_f(s) &= a_f^Z(s) - a_f^\gamma \frac{\Sigma_{\gamma Z}(s)}{s + \Sigma_{\gamma\gamma}(s)}, \end{aligned} \quad (12)$$

where v_f^X and a_f^X are the effective vector and axial-vector couplings of vertices $Xf\bar{f}$, and the self-energy Σ_{XY} stems from $\gamma - Z$ mixing at higher-orders.

2.2.3 Partial Width $\bar{\Gamma}[Z \rightarrow f\bar{f}]$

the partial width $\bar{\Gamma}$ can be recast by the Z-boson self-energy and vector/axial-vector couplings by applying optical theorem. It reads

$$\bar{\Gamma}_f = \frac{N_c^f \bar{M}_Z}{12\pi} C_Z [\mathcal{R}_V^f |V_f|^2 + \mathcal{R}_A^f |A_f|^2]_{s=\bar{M}_Z^2}. \quad (13)$$

Here $N_c^f = 3(1)$ for quarks(leptons), and C_Z is given by Z self-energy contributions at given orders. The radiators $\mathcal{R}_{V,A}$ contain final-state QCD and QED radiations. In our case, when only closed fermionic loops are considered, they are simply 1.

3 Technical Aspects

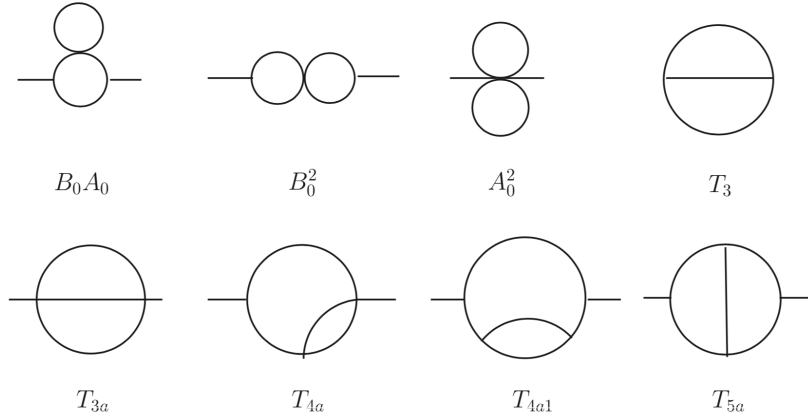


Figure 2: The MI topologies used for genuine two-loop self-energy contributions, with notation taken from [31].

In this calculations we turned off CKM mixing and all fermion masses, except the top quark, due to their negligible numerical impact. FEYNARTS 3.3 [26] and FEYNCALC 9.2.0 [27] are employed for amplitudes generation and algebraic reduction. The numerical evaluation is carried out by using TVID 2.0 [31]. Some $\mathcal{O}(D-4)$ coefficients from scalar one-loop integrals have been computed by following Eq. 4.1 in Ref. [33]. When comparing with previous results with two fermionic loops in Refs. [2, 3], [6] and [9], we have found exact algebraic agreement except one term

$$-\frac{d}{ds} \left(\frac{[\mathfrak{I}\Sigma_{\gamma Z(1)}(s)]^2}{s} \right), \quad (14)$$

which stems from $\gamma - Z$ mixing at two-loop level in partial Z width, which was missing in Ref. [9]. In Ref. [20], this error has been corrected and its numerical impact was evaluated.

For genuine two-loop amplitudes, the MI reductions are done in two independent ways: integration-by-part (IBP) identities [28] as implemented in FIRE6 [29], and the integral reduction techniques of Ref. [30]. We should mention that, unlike one-loop cases, the choice of a MI basis at the two-loop level is not unique and may also not be minimal. One of the MI bases used in this calculation is shown in Fig 2. However, despite the different choices of the MI basis, the two independent calculations by the authors agree numerically. Furthermore,

one must also compute the derivatives of two-loop self-energy functions to carry out the necessary renormalization counterterms. Care must be taken when deriving the derivative of the two-loop self-energy master integral with zero external momentum. With the help of chain rules, we obtain

$$\begin{aligned} \frac{\partial}{\partial p^2} I(\dots; p^2 = 0) &= \frac{1}{2d} \frac{\partial^2}{\partial p_\mu \partial p^\mu} I(\dots; p^2) \Big|_{p^2=0} \\ &= \frac{2}{d} \left[\left(1 + a_2 + a_5 - \frac{d}{2}\right) (a_2 \mathbf{2}^+ + a_5 \mathbf{5}^+) \right. \\ &\quad + m_2^2 a_2 (a_2 + 1) \mathbf{2}^{++} + m_5^2 a_5 (a_5 + 1) \mathbf{5}^{++} \\ &\quad \left. + a_2 a_5 ((m_2^2 - m_3^2 + m_5^2) \mathbf{2}^+ \mathbf{5}^+ - \mathbf{2}^+ \mathbf{3}^- \mathbf{5}^+) I \right]_{p^2=0}, \end{aligned} \quad (15)$$

whereas for $p^2 \neq 0$, one obtains [9]

$$\begin{aligned} \frac{\partial}{\partial p^2} I(\dots; p^2 \neq 0) &= -\frac{1}{2p^2} p^\mu \frac{\partial}{\partial p^\mu} I(\dots; p^2) \\ &= -\frac{1}{2p^2} \left[(a_2 + a_5) - a_2 \mathbf{1}^- \mathbf{2}^+ - a_5 \mathbf{4}^- \mathbf{5}^+ \right. \\ &\quad \left. + a_2 (m_2^2 - m_1^2 + p^2) \mathbf{2}^+ + a_5 (m_5^2 - m_4^2 + p^2) \mathbf{5}^+ \right] I, \end{aligned} \quad (16)$$

where I is defined as the most generic two-loop self-energy master integral

$$\begin{aligned} &I(a_1, a_2, \dots, m_1, m_2, \dots; p^2) \\ &\equiv \int \frac{d^d q_1 d^d q_2}{(q_1^2 - m_1^2)^{a_1} ((q_1 + p)^2 - m_2^2)^{a_2} ((q_2 - q_1)^2 - m_3^2)^{a_3} (q_2^2 - m_4^2)^{a_4} ((q_2 + p)^2 - m_5^2)^{a_5}} \end{aligned} \quad (17)$$

and the standard lowering/raising operators are defined as

$$\mathbf{4}^- \mathbf{5}^+ I = I(a_4 - 1, a_5 + 1). \quad (18)$$

Then one can apply IBP identities again to further reduce the raised/lowered MI integrals $I(\dots; p^2)$ down to the chosen MI basis such as Fig. 2.

4 Numerical Results

Given the benchmark inputs in Tab. 1, the numerical results for the leading fermionic contributions to all above-mentioned EWPOs at both $\mathcal{O}(\alpha^3)$ and mixed EW-QCD $\mathcal{O}(\alpha^2 \alpha_s)$ are shown in Tab. 2. It is evident that all the corrections computed at leading fermionic three-loop level are negligible for the precision tests conducted at the LEP and LHC, see Tab. 3. However, one can also see that the experimental uncertainties mapped out by future e^+e^- colliders are comparable to the three-loop corrections. Hence these corrections computed in Ref. [20] cannot be ignored. Combining the $\mathcal{O}(\alpha^3)$ and $\mathcal{O}(\alpha^2 \alpha_s)$ corrections, we see $\Delta \overline{M}_W$ and $\Delta \overline{\Gamma}$ having a sizable corrections while others are subject to accidental cancellations. When switching the top-quark mass from OS to $\overline{\text{MS}}$ prescription, using the benchmark value given in Tab. 1, the overall magnitude of leading fermionic $\mathcal{O}(\alpha^2 \alpha_s)$ corrections become noticeably smaller. This is normally expected as $\overline{\text{MS}}$ prescription converges faster than OS for QCD corrections. We perform the similar numerical evaluations summarized in Tab. 4.

A thorough comparison between OS and $\overline{\text{MS}}$ top mass prescription is given in Ref. [20] Tab.5, from which one observes that the numerical shifts at two-loop and three-loop levels partially compensate each other in both schemes as one would expect.

$M_Z = 91.1876 \text{ GeV}$	}	$\Rightarrow \bar{M}_Z = 91.1535 \text{ GeV}$
$\Gamma_Z = 2.4952 \text{ GeV}$		
$M_W = 80.358 \text{ GeV}$	}	$\Rightarrow \bar{M}_W = 80.331 \text{ GeV}$
$\Gamma_W = 2.089 \text{ GeV}$		
$M_t = 173.0 \text{ GeV}$		
$m_t(\mu = m_t) = 163.229 \text{ GeV.}$		
$M_{f \neq t} = 0$		
$\alpha_s = 0.1179$		
$\alpha = 1/137.035999084$		
$\Delta\alpha = 0.05900$		
$G_\mu = 1.1663787 \times 10^{-5} \text{ GeV}^{-2}$		

Table 1: Benchmark input parameters used in the numerical analysis, based on Ref. [16]. Both benchmark values for alternative top-quark mass prescriptions are listed.

	Δr	$\Delta \bar{M}_W$ (MeV)	$\Delta \sin^2 \theta_{\text{eff}}$	$\Delta' \sin^2 \theta_{\text{eff}}$	$\Delta \bar{\Gamma}_{\text{tot}}$ [MeV]	$\Delta' \bar{\Gamma}_{\text{tot}}$ [MeV]
$\mathcal{O}(\alpha^3)$	2.5×10^{-5}	-0.389	1.34×10^{-5}	2.09×10^{-5}	0.331	0.255
$\mathcal{O}(\alpha^2 \alpha_s)$	-0.000109	1.703	1.31×10^{-5}	-1.98×10^{-5}	-0.103	0.229
Sum	-0.000084	1.314	2.65×10^{-5}	0.11×10^{-5}	0.228	0.484

Table 2: This table shows the numerical results of the leading fermionic three-loop corrections to EWPOs at $\mathcal{O}(\alpha^3)$ and at $\mathcal{O}(\alpha^2 \alpha_s)$ from Ref. [20]. The EWPOs denoted with a prime use M_W predicted from the Fermi constant G_μ rather than the value in Tab. 1. One can see that the two contributions have comparable size, except for $\Delta \bar{M}_W$, where the mixed EW-QCD three-loop correction is about four times larger in magnitude than the pure EW three-loop.

As mentioned above, a previous paper has missed the term (14) contributing to $\Delta \bar{\Gamma}_f$ at two-loop order. This missing term results in numerical impact around $\mathcal{O}(0.01)$ MeV to $\Delta \bar{\Gamma}_f$. This turns out to be relatively small but clearly non-negligible for the precision level we want to achieve at future colliders.

5 Conclusions

In this proceeding, we highlight recent computations of leading fermionic three-loop corrections to EWPOs at both $\mathcal{O}(\alpha^3)$ and mixed EW-QCD $\mathcal{O}(\alpha^2 \alpha_s)$. These computations are carried out in a fully gauge-invariant way. The numerical size of leading fermionic loop corrections should be considerably large due to the power of top mass and N_f^n enhancement. However, they turn out to be milder than one would expect due to some accidental cancellations. Hence, other missing three-loop contributions may give corrections of similar magnitude, and they need to be included to further reduce the intrinsic theoretical uncertainty down to the level that matches the goals of future colliders. Here genuine electroweak three-loop integrals with various scales in the denominators will come into play, which will require significant additional work in the future.

	Global fits at LEP/SLD/LHC	Current intrinsic theo. error	CEPC	FCC-ee	ILC/GigaZ
M_W [MeV]	12	$4(\alpha^3, \alpha^2\alpha_s)$	1	$0.5 \sim 1$	2.5
Γ_Z [MeV]	2.3	$0.4(\alpha^3, \alpha^2\alpha_s, \alpha\alpha_s^2)$	0.5	0.1	1.0
$\sin^2 \theta_{\text{eff}}^f$ [10^{-5}]	16	$4.5(\alpha^3, \alpha^2\alpha_s)$	2.3	0.6	1

Table 3: This table demonstrates the current experimental uncertainties given by the global fits of measurements taken from the LEP, SLD, and LHC vs. future experimental accuracies projected for CEPC, FCC-ee, and ILC for three EWPOs [21–24]. For ILC, the GigaZ option is considered, which is a Z-pole run with 100 fb^{-1} .

X	$\Delta X_{(\alpha^2\alpha_s)}$	$\Delta' X_{(\alpha^2\alpha_s)}$
Δr [10^{-4}]	−0.50	
ΔM_W [MeV]	0.78	
$\sin^2 \theta_{\text{eff}}^f$ [10^{-5}]	0.75	−0.76
Γ_{tot} [MeV]	−0.0093	0.143

Table 4: Leading fermionic three-loop corrections to EWPOs at $\mathcal{O}(\alpha^2\alpha_s)$ with \overline{MS} prescription for the top mass.

Acknowledgements

This work has been supported in part by the National science Foundation under grant no. PHY-1820760.

References

- [1] A. Djouadi and C. Verzegnassi, Phys. Lett. B **195**, 265 (1987);
A. Djouadi, Nuovo Cim. A **100**, 357 (1988);
B. A. Kniehl, Nucl. Phys. B **347**, 86 (1990);
B. A. Kniehl and A. Sirlin, Nucl. Phys. B **371**, 141 (1992);
A. Djouadi and P. Gambino, Phys. Rev. D **49**, 3499 (1994) [Erratum-ibid. D **53**, 4111 (1996)] [hep-ph/9309298].
- [2] A. Freitas, W. Hollik, W. Walter and G. Weiglein, Phys. Lett. B **495**, 338 (2000) [Erratum-ibid. B **570**, 260 (2003)] [hep-ph/0007091].
- [3] A. Freitas, W. Hollik, W. Walter and G. Weiglein, Nucl. Phys. B **632**, 189 (2002) [Erratum-ibid. B **666**, 305 (2003)] [hep-ph/0202131].
- [4] M. Awramik and M. Czakon, Phys. Rev. Lett. **89**, 241801 (2002) [hep-ph/0208113],
Phys. Lett. B **568**, 48 (2003) [hep-ph/0305248];
A. Onishchenko and O. Veretin, Phys. Lett. B **551**, 111 (2003) [hep-ph/0209010].
- [5] M. Awramik, M. Czakon, A. Freitas and G. Weiglein, Phys. Rev. D **69**, 053006 (2004) [hep-ph/0311148].
- [6] M. Awramik, M. Czakon, A. Freitas, G. Weiglein, Phys. Rev. Lett. **93**, 201805 (2004) [hep-ph/0407317].

- [7] M. Awramik, M. Czakon and A. Freitas, Phys. Lett. B **642**, 563 (2006) [hep-ph/0605339], JHEP **0611**, 048 (2006) [hep-ph/0608099]; W. Hollik, U. Meier and S. Uccirati, Nucl. Phys. B **731**, 213 (2005) [hep-ph/0507158], Nucl. Phys. B **765**, 154 (2007) [hep-ph/0610312].
- [8] M. Awramik, M. Czakon, A. Freitas and B. A. Kniehl, Nucl. Phys. B **813**, 174 (2009) [arXiv:0811.1364 [hep-ph]].
- [9] A. Freitas, Phys. Lett. B **730**, 50 (2014) [arXiv:1310.2256 [hep-ph]], JHEP **1404**, 070 (2014) [arXiv:1401.2447 [hep-ph]].
- [10] I. Dubovyk, A. Freitas, J. Gluza, T. Riemann and J. Usovitsch, Phys. Lett. B **762**, 184 (2016) [arXiv:1607.08375 [hep-ph]], Phys. Lett. B **783**, 86 (2018) [arXiv:1804.10236 [hep-ph]], JHEP **1908**, 113 (2019) [arXiv:1906.08815 [hep-ph]].
- [11] L. Avdeev, J. Fleischer, S. Mikhailov and O. Tarasov, Phys. Lett. B **336**, 560 (1994) [Erratum-ibid. B **349**, 597 (1994)] [hep-ph/9406363]; K. G. Chetyrkin, J. H. Kühn and M. Steinhauser, Phys. Lett. B **351**, 331 (1995) [hep-ph/9502291]; Phys. Rev. Lett. **75**, 3394 (1995) [hep-ph/9504413].
- [12] J. J. van der Bij, K. G. Chetyrkin, M. Faisst, G. Jikia and T. Seidensticker, Phys. Lett. B **498**, 156 (2001) [hep-ph/0011373]; M. Faisst, J. H. Kühn, T. Seidensticker and O. Veretin, Nucl. Phys. B **665**, 649 (2003) [hep-ph/0302275].
- [13] Y. Schröder and M. Steinhauser, Phys. Lett. B **622**, 124 (2005) [hep-ph/0504055]; K. G. Chetyrkin, M. Faisst, J. H. Kühn, P. Maierhofer and C. Sturm, Phys. Rev. Lett. **97**, 102003 (2006) [hep-ph/0605201]; R. Boughezal and M. Czakon, Nucl. Phys. B **755**, 221 (2006) [hep-ph/0606232].
- [14] A. Freitas, Prog. Part. Nucl. Phys. **90**, 201 (2016) [arXiv:1604.00406 [hep-ph]].
- [15] J. Erler and M. Schott, Prog. Part. Nucl. Phys. **106**, 68 (2019) [arXiv:1902.05142 [hep-ph]].
- [16] See J. Erler and A. Freitas, section 10 of M. Tanabashi *et al.* [Particle Data Group], Phys. Rev. D **98**, 030001 (2018) [pdg.lbl.gov/2019/reviews/rpp2018-rev-standard-model.pdf].
- [17] S. Willenbrock and G. Valencia, Phys. Lett. B **259**, 373 (1991); A. Sirlin, Phys. Rev. Lett. **67**, 2127 (1991); R. G. Stuart, Phys. Lett. B **262**, 113 (1991); H. G. J. Veltman, Z. Phys. C **62**, 35 (1994).
- [18] D. Y. Bardin, A. Leike, T. Riemann and M. Sachwitz, Phys. Lett. B **206**, 539 (1988).
- [19] R. Tarrach, Nucl. Phys. B **183**, 384-396 (1981); N. Gray, D. J. Broadhurst, W. Grafe and K. Schilcher, Z. Phys. C **48**, 673-680 (1990); K. G. Chetyrkin and M. Steinhauser, Nucl. Phys. B **573**, 617-651 (2000) [arXiv:hep-ph/9911434 [hep-ph]]; K. Melnikov and T. v. Ritbergen, Phys. Lett. B **482**, 99-108 (2000) [arXiv:hep-ph/9912391 [hep-ph]]; P. Marquard, L. Mihaila, J. H. Piclum and M. Steinhauser, Nucl. Phys. B **773**, 1-18 (2007) [arXiv:hep-ph/0702185 [hep-ph]]; P. Marquard, A. V. Smirnov, V. A. Smirnov and M. Steinhauser, Phys. Rev. Lett. **114**, no.14, 142002 (2015) [arXiv:1502.01030 [hep-ph]].

- M. Fael, F. Lange, K. Schönwald and M. Steinhauser, doi:10.1007/JHEP09(2021)152 [arXiv:2106.05296 [hep-ph]].
- [20] L. Chen and A. Freitas, JHEP **07**, 210 (2020) [arXiv:2002.05845 [hep-ph]].
JHEP **03**, 215 (2021) [arXiv:2012.08605 [hep-ph]].
- [21] J. B. Guimares da Costa *et al.* [CEPC Study Group], arXiv:1811.10545 [hep-ex].
- [22] A. Abada *et al.* [FCC Collaboration], Eur. Phys. J. ST **228**, 261 (2019).
- [23] K. Fujii *et al.* [LCC Physics Working Group], arXiv:1908.11299 [hep-ex].
- [24] G. W. Wilson, [arXiv:1603.06016 [hep-ex]].
- [25] F. Jegerlehner, EPJ Web Conf. **218**, 01003 (2019) [arXiv:1711.06089 [hep-ph]];
M. Davier, A. Hoecker, B. Malaescu and Z. Zhang, Eur. Phys. J. C **80**, no.3, 241 (2020)
[erratum: Eur. Phys. J. C **80**, no.5, 410 (2020)] [arXiv:1908.00921 [hep-ph]].
A. Keshavarzi, D. Nomura and T. Teubner, Phys. Rev. D **101**, no.1, 014029 (2020)
[arXiv:1911.00367 [hep-ph]].
- [26] T. Hahn, Comput. Phys. Commun. **140**, 418 (2001) [hep-ph/0012260].
- [27] V. Shtabovenko, R. Mertig and F. Orellana, Comput. Phys. Commun. **207**, 432 (2016)
[arXiv:1601.01167 [hep-ph]].
- [28] K. G. Chetyrkin and F. V. Tkachov, Nucl. Phys. B **192**, 159-204 (1981).
- [29] A. V. Smirnov and F. S. Chuharev, arXiv:1901.07808 [hep-ph].
- [30] G. Weiglein, R. Scharf and M. Böhm, Nucl. Phys. B **416**, 606-644 (1994) [arXiv:hep-ph/9310358 [hep-ph]].
- [31] S. Bauberger, A. Freitas and D. Wiegand, JHEP **01**, 024 (2020) [arXiv:1908.09887 [hep-ph]].
- [32] A. Freitas, Diploma thesis, University of Karlsruhe (1999)
[www.itp.kit.edu/prep/diploma/PSFiles/diploma-2-1999.ps.gz].
- [33] U. Nierste, D. Muller and M. Böhm, Z. Phys. C **57**, 605-614 (1993).
- [34] A. Blondel *et al.*, arXiv:1809.01830 [hep-ph].